Transcriptomic analysis reveals the molecular mechanisms of wheat seedling resistance to *Puccinia striiformis* f. sp. *tritici*

Rong Liu
University of Chinese Academy of Sciences
Jing Lu
University of Chinese Academy of Sciences
Mei Du
University of the Chinese Academy of Sciences
Min Zhou
University of the Chinese Academy of Sciences
Mingxiu Wang
University of the Chinese Academy of Sciences
Jiayi Xing
University of the Chinese Academy of Sciences
Chihong Zhang
University of the Chinese Academy of Sciences
Yunfang Li
University of the Chinese Academy of Sciences
Yu Wu
University of the Chinese Academy of Sciences
Lei Zhang (L95620@126.com)
Chengdu Institute of Biology, Chinese Academy of Sciences

Research article

Keywords: Wheat, stripe rust, yellow rust, CYR34, transcriptome, resistance gene pyramiding

Posted Date: February 5th, 2020

DOI: https://doi.org/10.21203/rs.2.22691/v1

Abstract

Background: Stripe rust or yellow rust (*Yr*), caused by *Puccinia striiformis* f. sp. *Tritici* (*Pst*), is one of the most globally devastating fungal disease that significantly reduces yield and quality in wheat (*Triticum aestivum*). Although some *Yr* genes have been successfully used in wheat breeding and a little number of them have been cloned, large of the regulating networks and the molecular mechanisms of *Pst* resistance remains unknown. In this study, a pair of *Yr*-gene pyramiding line L58 and its background parent cv. Chuanyu12 (CY12) were used to study the transcriptome profiles after inoculated with *Pst* physiological race *CYR34*.

Results: The results revealed that the different expression genes (DEGs) were significantly enriched in phenylpropanoid biosynthesis, phenylalanine metabolism, plant-pathogen interaction and MAPK signaling pathways after *Pst-CYR34* inoculation. Compared with CY12, L58 showed greater up-regulated DEGs in those pathways by *Pst* infection at 24hpi. However, these DEGs became lower expression in L58 and opposite expression in CY12 at 7dpi. Besides, the activities of enzymes (PAL, POD) and products of phenylpropanoid pathway (lignin content) were significantly increased in both CY12 and L58, and the increase was greater and faster in the resistant line L58. Some candidate genes and transcription factors (TFs) associated with *Pst* resistance were identified, including LRR receptor-like serine/threonine protein kinase, disease resistance protein, MYB, NAC and WRKY transcription factors involved in the fine-tuning of *Pst* infection responses.

Conclusions: Our results give insights into the regulating networks of *Pst* resistance and pave the way for durable resistant breeding in bread wheat.

Background

Wheat (*Triticum aestivum* L.) has been a major staple food crop in the world over the centuries [1, 2]. Plants are constantly exposed to microbes in ecosystem[3]. Stripe or yellow rusts (*Yr*) of wheat caused by *Puccinia striiformis* f. sp. *tritici* (*Pst*), is one of the most globally devastating fungal disease in wheat[4, 5], which can cause massive yield losses in wheat. Those pathogens are capable spreading for a long-distance through seasonal wind and human-assisted movement among continents[2]. Stripe rust threatens all winter wheat cultivars and has been considered as the most important fungal disease to decrease wheat production in China[6, 7]. As the stripe rust pathogens have strong adaptive capacity and evolve rapidly, the resistance of a newly released variety usually lasts for only several years [8]. Then the resistance ineffective will render an increase in area of replacement variety resistant to the new virulent race. The “boom and bust cycle” is more common in varieties released carrying single major genes[9]. For example, a new *Pst* race group (*V26*/*CYR34*) which was virulent to resistance gene *Yr26* has spread in several major wheat growing regions where *Yr26* was widely used in the wheat breeding programs[10-12]. Recently, some study reported that most of current wheat cultivars and breeding lines (76%) are susceptible to *CYR34*[13]. Wheat cultivars with *Yr26* is still distributing predominantly frequently in China,

so it's necessary to breed novel resistant cultivars before *CYR34* bringing more lost in wheat production[5].

There are nine disease resistance mechanisms in plant species, the classic model is mainly pathogen-associated molecular pattern-triggered immunity (PTI) and effector-triggered immunity (ETI) systems. The main difference between the two modes is that the latter triggers an allergic necrosis or hypersensitivity reaction (HR). Plants have a defensive response to pathogen attack mediating by resistance genes to delay or prevent the growth of potential pathogenic microorganisms[14] through PTI and ETI systems. The current analysis of plant immunity has evolved towards a comprehensive view of plant-pathogen interactions[15]. Global gene expression methods can be used to elucidate the molecular mechanisms of wheat-fungal interactions, particularly the use of next-generation sequencing technologies to study important non-model hosts-pathogen systems such as wheat rust[16]. A large number of researches on wheat-rust interactions have been carried out by Affymetrix® GeneChip® Wheat Genome Array (Affymetrix, Santa Clara, CA, USA)[17, 18] and cDNA-AFLP analysis[19]. However, compared with other plants using genetic and molecular techniques to study genes associated with wheat-*Pst* interactions has been limited[20]. The gene expression profile for the response to the stripe rust races in the both resistant and susceptible wheat is still lacking and large of the regulating networks and the molecular mechanisms of *Pst* resistance remains unknown.

Until now, *Yr1~Yr80* have been reported and most of them have been used for breeding programs of stripe rust resistance[21]. However, only a few *Yr* genes (*Yr5*, *Yr15*, *Yr18* and *Yr65*) have maintained field resistance to rust fungi [22, 23]. Therefore, the most effective, low-cost and environmentally safe way to control stripe rust is rationally distributing *Yr* genes in different wheat regions or breeding wheat cultivars with durable and broad-spectrum resistance[24]. Besides, many studies have reported that resistance gene pyramiding was an effective way for "durable" controlling crop diseases to achieve broad-spectrum and long-lasting resistance to protect crops from pathogens [25, 26]. In this study, the phenotypic and transcriptomic responses of wheat cv. Chuanyu12 (CY12) and resistance breeding line L58 (pyramiding with *Yr10*, *Yr15*, *Yr30* and *Yr65*) were investigated under *Pst-CYR34* inoculation of the Gansu Academy of Agricultural Sciences (GAAS). Furthermore, the metabolites accumulation and key enzymes activity were determined under *Pst* infection to verify the accuracy of gene expression in *Pst* responses signal pathways. To reveals the molecular mechanisms of wheat resistance to *Puccinia striiformis* f. sp. *tritici*.

Methods

Plant materials and fungal treatment

The wheat cv. CY12 and pyramiding line L58 were used in this study, which obtained from Chengdu Biology of Sciences, Chinese Academy of Sciences. CY12 is developed by our research group and highly susceptible to currently predominant stripe rust. L58 is a pyramiding line (*Yr10*, *Yr15*, *Yr30* and *Yr65*) with CY12 as background which shows high resistance to new *Pst*-race *CYR34* in our previous research[39]. Artificial inoculation at Seedling stage was conducted under a controlled greenhouse condition in Gansu

Academy of Agricultural Sciences (GAAS). Two-week old seedlings were inoculated with *Pst-CYR34*. The wheat cv. Mingxian169 was used to monitor inoculation efficiency. The wheat leaves of CY12 and L58 were collected at 0h (a), 24h (b), and 7 days (c) post-inoculation (each time point with 3 biological replicates). All leaf samples were frozen in liquid nitrogen and stored in a −80°C refrigerator for transcriptome sequencing. After the wheat varieties Mingxian169 and CY12 were fully sporulating, then the samples were used for experiment.

RNA Isolation and cDNA library construction for RNA Sequencing

Total RNA of wheat leaves was extracted using the mirVana miRNA Isolation Kit (Ambion) following the manufacturer's protocol. RNA integrity was evaluated using the Agilent 2100 Bioanalyzer (Agilent Technologies, Santa Clara, CA, USA). The samples with RNA Integrity Number (RIN) ≥7 were subjected to the subsequent analysis. Total RNA from the wheat leaves was to break into short fragments at a suitable temperature in the thermomixer. Then purified fragment mRNA was used to synthesize first strand cDNA and second strand cDNA. The libraries were constructed using TruSeq Stranded mRNA LTSample Prep Kit (Illumina, San Diego, CA, USA) according to the manufacturer's instructions. Then 18 cDNA libraries were sequenced on the Illumina sequencing platform (HiSeqTM 2500 or Illumina HiSeq X Ten) and 125bp/150bp paired-end reads were generated.

The transcriptome sequencing and analysis were conducted by OE biotech (Shanghai, China). Raw data (raw reads) were processed using Trimmomatic[27]. The reads containing ploy-N and the low quality reads were removed to obtain the clean reads. Then, all clean reads used to subsequent analyses and mapped to reference genome using hisat2[28].

Differential expression genes (DEGs), Gene Ontology (GO) and KEGG Analysis

FPKM[29] value of each gene was calculated using cufflinks[30], and the read counts of each gene were obtained by htseq-count[31]. Differentially expressed genes (DEGs) were analysis and identified using the DEGseq R package. DEGs were selected with a |log2 FC|>1 and Q<0.005 as the thresholds, which tested whether each gene was affected by genotype and time point. Hierarchical cluster analysis of DEGs was performed to explore genes expression pattern. And P values were adjusted using the Benjamini-Hochberg correction for multiple testing[32]. GO enrichment and KEGG[33] pathway enrichment analysis of DEGs were respectively performed using R based on the hypergeometric distribution during *CYR34* infection.

Weighted gene correlation network analysis (WGCNA)

Co-expression networks were constructed using the WGCNA R software package with a soft thresholding power of 10[34]. 14979 assembled genes were selected with FPKM>5 for the WGCNA unsigned co-expression network analysis. The total connectivity, intramodular connectivity (function soft Connectivity), kME (for modular membership, i.e., eigengene-based connectivity), and kME-p-values were

calculated for all 14979 genes. Hub genes with potentially important functions were identified as those with high connectivity.

Determination of lignin content and enzyme activities

L58 and CY12 wheat leaves were collected at 0hpi, 24hpi and 7dpi. The lignin content was determined by the lignin-thioglycolic acid (LTGA) reaction[35]. The determination of PAL activity was performed according to the Li et al. 2011[36]. And peroxidase (POD) activity was measured by the increase in absorbance at 470nm[37].

qRT-PCR analysis

Sixteen DEGs were randomly selected for qRT-PCR analysis, and GAPDH was used as the internal reference gene. The primers were designed based on the sequence of genes using Primer 5.0 and are listed in Table S1. The RNA extracted from CY12 and L58 wheat seedlings at 0h, 24h and 7days were used to synthesize first-strand cDNA with HiScriptII Q RT SuperMix (Vazyme, R223-1) following the manufacturer's instructions. The qRT-PCR was performing with SYBR® Green PCR kit (Qiagen, 204054) according to the manufacturer's instructions. The experimental conditions were set as follows: 45 cycles at 95 °C for 20 s, 55 °C for 20 s, and 72 °C for 20 s. All genes were repeated 3 times in this study. The mRNA expression level of the genes were calculated with the $2^{-\Delta\Delta Ct}$ method[38]. Each wheat leaf sample was repeated 3 times. The correlation between RNA-seq and qRT-PCR results was analyzed using these values R package version 3.1.3 (http://cran.r-project.org/). The normalized values of relative expression and RPKM values were calculated using log2 (fold change) measurements.

Statistical analysis of data

Data of three biological repeats were analyzed using GraphPad Prism 5, Excel 2013 and SPSS 20.0 and rendered as means ± SD. One-way ANOVA followed by Tukey's significant difference test at $p<0.05$. All data had 3 biological repeats. Differentially expressed genes were defined as genes with FDR<0.001 and fold change >2-fold. A p-value < 0.05 was considered significant when identifying enriched GO terms, and a p-value < 0.05 was considered indicative of significantly enriched KEGG pathways.

Results

Phenotype identification of two wheat after *Pst* infection

Two-week old wheat seedling leaves of Chuanyu12 (CY12)、L58 and Mingxian169 were inoculated with *Pst-CYR34*, and incubation in dark room for 24h. Different responses to the *Pst* infection were observed in CY12 (susceptible) and L58 (resistance) at seedling stage and adult-plant stage (Figure 1). L58 is offspring of CY12, and in previous study we use molecular assistant selection to detected four *Yr* genes (*Yr10*, *Yr15*, *Yr30* and *Yr65*) in L58 which located on B chromosome[39].

Wheat mRNA transcriptome and analysis

To further elucidate the molecular basis for the differential stripe rust response in CY12 and L58, comparative transcriptome analysis was conducted through RNA sequencing. Both the 24-h and 7-day *Pst* treatments were used to investigate early and later response of wheat to *Pst-CYR34*. Eighteen cDNA libraries, each for CY12 and L58 inoculated with *Pst-CYR34* and non-infected control at two time points, were characterized by Illumina HiSeq to detect the transcriptome level of gene expression information. After removing low-quality reads and those containing adapter and ploy-N, about 48.0 million (range 47.02 to 48.62) clean reads were obtained in per library, among which more than 86.55% clean reads per library could be mapped to the wheat reference genome (ftp://ftp.ensemblgenomes.Org/pub/plants/release-37/fasta/triticum_aestivum/dna/Triticum_aestivum.TGACv1.dna.toplevel.fa.gz). The uniquely mapped in CY12_a (0hpi), CY12_b (24hpi), CY12_c (7dpi), L58_a (0hpi), L58_b (24hpi), and L58_c (7dpi) was (86.92±0.35)%, (97.64±0.2)%, (86.55±0.45)%, (86.61±0.16)%, (87.93±0.12)% and (86.48±1.19) %, respectively (Table 1).

DEGs identification

The DEGs were identified by comparing the FPKMs values of each gene between CY12 and L58 (with 0, 24hpi and 7dpi) with the criteria of fold change≥2 and $P < 0.05$. Then DEGs involved in *Pst-CYR34* infection process were screened. There were 4607 differentially expressed genes between CY12 and L58 with non-*Pst* infection, while the number of DEGs changed to 4834 and 4456 after 24hpi and 7dpi with *CYR34* treatment, respectively (Figure 2A). The DEGs of two wheat lines CY12 and L58 treatments with *Pst-CYR34* were found for 4607 DEGs (2592 up-regulated and 2015 down-regulated) in L58_a vs CY12_a, 4834 DEGs (2721 up-regulated and 2113 down-regulated) in L58_b vs CY12_b and 4456 DEGs (2252 up-regulated and 2204 down-regulated) in L58_c vs CY12_c (Figure 2B). All up-regulated DEGs and down-regulated DEGs at 0hpi, 24hpi and 7dpi were shown in Figure 2C, 2D.

Verification of RNA-Seq by qRT-PCR

To evaluate the validity of transcriptome profiles from the RNA sequencing analysis, 16 *Pst-CYR34* induced genes were randomly selected for qRT-PCR expression analysis. The correlation of RNA-Seq (FPKM) and qRT-PCR are shown in Figure 3 (Supplemental File 1-1). The relative expression levels of the genes from qRT-PCR were consistent with those from the RNA-Seq data. And there have a significantly positive correlation between RNA-Seq and qRT-PCR results, the correlation coefficient was $r=0.95$ ($P < 0.001$), which confirming the reliability of the RNA-Seq data.

GO enrichment and KEGG analysis of DEGs

The DEGs have contributed to the phenotypic differences in *Pst-CYR34* infection between CY12 and L58. To identify the major functional terms under the *Pst-CYR34* treatment, GO enrichment analysis was carried out of DEGs (Figure 4A). GO enrichment results showed that *Pst-CYR34* related DEGs were mainly enriched in metabolic process, cellular process, response to stimulus and biological regulation in the

biological process; also associated with cell part, organelle part and membrane part in the cellular component; and catalytic activity, binding and transporter activity in the molecular function category.

DEGs were also enriched in KEGG pathways in this study. For the 24hpi, *Pst-CYR34* induced DEGs in CY12 and L58 were notably enriched in necroptosis (KO 04217), plant-pathogen interaction (KO 04626), ribosome (KO 03010), MAPK signaling pathway-plant (KO 04016), phenylpropanoid biosynthesis (KO 00940) and phenylalanine metabolism (KO 00360)(Figure 4B). Thirty-eight DEGs were enriched in the plant-pathogen interaction pathway, among them 31 up-regulate and only 7 DEGs down under the *Pst-CYR34* treatment. MAPK signaling pathway enriched 44 DEGs that 39 were up and 5 down regulation at 24hpi. Those up regulated gene including certain key enzyme genes or TFs, such as *WRKY33*, *ANP1*, *SNRK2*, *PR1* and *ERF1* et al. Similarly, 69 DEGs in the phenylpropanoid biosynthesis have 60 DEGs up-regulated, including PAL, E1.11.1.7, PTAL, COMT, REF1, etc. Phenylalanine metabolism as the upstream pathway of phenylpropanoid biosynthesis, most DEGs were also up-regulated, including enzyme encoding genes amiE and MIF, etc (Figure 4C). The up-regulated genes in this pathway also prepares for substance synthesis in the downstream pathway. For the 7dpi of *Pst-CYR34* induced DEGs in CY12 and L58 were enriched in glutathione metabolism (KO 00480), porphyrin and chlorophyll metabolism (KO 00860), alanine, aspartate and glutamate metabolism (KO 00250), phenylalanine metabolism (KO 00360), sulfur metabolism (KO 00920), carotenoid biosynthesis (KO 00906), phenylpropanoid biosynthesis (KO 00940), flavonoid biosynthesis (KO 00941), cysteine and methionine metabolism (KO 00270) and plant-pathogen interaction et al. (Figure 4D). Those results indicate that plant-pathogen interaction, phenylpropanoid biosynthesis and MAPK signaling pathway are important for defense response or disease resistance in wheat.

Lignin accumulation in wheat to resistant *Pst-CYR34*

The *Pst* induced DEGs involved in phenylpropanoid biosynthesis were examined in this study. Figure 5A (Supplemental File 1-2) shows the heat map of DEGs in phenylpropanoid biosynthesis at 0hpi, 24hpi and 7dpi in CY12 and L58. Most DEGs were up-regulated in L58 compare CY12 after inoculation. However, the DEGs has oppositely expression pattern at 7dpi. Therefore, the detail of phenylpropanoid biosynthesis and the *Pst*-induced expression pattern changes of those DEGs in this pathway during the defense response of *Pst-CYR34* infection (Figure 5B).

In this study, firstly, phenylpropanoid biosynthesis phenylalanine, and then with different steps of the pathway catalyzed by four types of enzymes: ammonia lyase (PAL), hydroxycinnamoyl transferase (HCT), cinnamyl alcohol dehydrogenase (CAD) and E1.11.1.7. Finally, the pathway produces three types of monolignols polymerize to form lignin, such as guaiacyl (G), syringyl (S), and p-hydroxyphenyl (H) lignin. The expression levels of DEGs in this pathway were illustrated using a heat map (Figure 5B) and estimated by log2 (fold change). Although there were some cases of downregulation or non-significant upregulation for some of the genes at different time points, most of the four types of genes in this pathway were upregulated in L58 within 24hpi compared with the non-inoculated control. Generally, the

upregulation of phenylpropanoid biosynthesis genes began at 24hpi or earlier and the peaks of relative expression of these genes occurred at 24hpi.

Based on the upregulation of genes related to phenylpropanoid biosynthesis pathway, we determined activities of PAL and POD, and we also determined the changes of lignin content in wheat leaves at 0hpi, 24hpi and 7dpi (Figure 5CDE). The activities of PAL and POD were increased in both CY12 and L58 after *Pst-CYR34* inoculation. However, compare with CY12, both PAL and POD activities were higher in L58 after *Pst* infection. Compare to control (0hpi), lignin content increased by 56.5% and 60.7% in CY12 at 24hpi and 7dpi, respectively. In L58, the lignin content were increased by 65.6% and 75.6% at 24hpi and 7hpi, respectively. Furthermore, lignin content was higher in the L58 than CY12 after *Pst*-inoculation, indicating that *Pst-CYR34* inoculation increased lignin biosynthesis to response defenses and enhancing the resistance of wheat.

Pst-CYR34 induced DEGs in plant-pathogen interaction

KEGG enrichment analysis exhibited the different response of plant-*Pst* interaction in both CY12 and L58. At 24hpi, the DEGs enrichment in plant-pathogen interaction pathway were almost up-regulated in L58 compare CY12. And adversely expression trend at 7dpi (Figure 6A). Of those DEGs at 24hpi in CY12 and L58 were showed in Figure 6B (Supplemental File 1-3). The up-regulated genes eventually involved to regulate ROS, defense-related gene induction, cell wall reinforment and hypersensitive response (HR) processes. This result indicate that the key period of plants to responses defense and is 24 hours post incubation. Otherwise, the plant will lose resistance by the pathogen successfully invading.

Pst-CYR34 induced DEGs involved in MAPK signaling pathway

MAPK signaling pathway was also important for CY12 and L58 to *Pst*-responsive DEGs. Those DEGs also up-regulated in L58 at 24hpi. However, at 7dpi the DEGs were mostly up-regulated in CY12 and those DEGs were already starting down expression in L58 at 7dpi (Figure 7A). These DEGs enrichment in MAPK signaling pathway exhibited in Figure 7B (Supplemental File 1-4). The *Pst-CYR34* stimuli by receptors and proteins anchored to the cell membrane, which directly activate a MAP kinase kinase kinase (MAPKKK) and in turn to activate a MAPKK (MAP kinase kinase) by phosphorylation of serine/threonine residues. Then, protein phosphorylates several MAP kinases, such as MPK3/6, MPK6 and MPK4/6 etc. Finally activate the transcription factors (PR1, WRKY33 and ERF1 etc.) to induce or repress genes expression involved in response to *Pst-CYR34* infection.

Weighted gene co-expression network analysis of wheat resistance to stripe rust

Co-expression network analysis was performed by weighted gene co-expression network analysis (WGCNA) which comparing 18 high-throughput RNA-Seq datasets generated from leaf samples under *Pst-CYR34* infection. In this study, a total 14,979 DEGs were identified for 18 samples at 0hpi, 24hpi and 7dpi. WGCNA was constructed on the basis of pairwise correlations between *Pst-CYR34* infection responsive genes using their common expression trends across all sample leaves. Based on the selected

power values, a weighted co-expression network model was established, and finally 14979 genes were divided into 16 modules. The gray cannot be attributed to any module and has no reference significance. The module eigengenes from the 16 main modules were correlated with distinct samples as sample-specific eigengene expression profiles in wheat responding to *Pst* (Figure 8A). Two of the co-expression modules: greenyellow and darkviolet consisted of genes that were highly expressed in wheat after *Pst*-infection($r > 0.6$, $p < 0.001$).

In these two modules, greenyellow comprised the most sample-specific expressed genes. These genes were enriched mainly in fatty acid metabolism, carbon metabolism, flavonoid biosynthesis, sulfur metabolism, fatty acid elongation metabolism and pentose phosphate pathway (Figure 8B, supplement file1-5). The Hub-genes in greenyellow and darkviolet modules were show in Figure 8C, D. The result suggest that greenyellow and darkviolet modules represent the primary gene expression module that characterized the specific response of CY12 and L58 to *Pst-CYR34*.

TFs and putative R genes in wheat associate with *Pst* response

In this study, 132 DEGs were identified as transcription factors (TFs) belonging to different families (WRKY, ERF, FAR1 and NAC, etc.). Of those TFs, 95 were up-regulated and 37 were down-regulated in wheat at 24hpi. WRKY was the TF family with the largest number of genes, flowed by NAC family, then was FAR1 and ERF TF families. Among the WRKY, ERF, FAR1 and NAC families mostly of genes were up-regulated in L58, while down-regulated in CY12 at 24hpi (Figure 9A, B, C, D, Supplemental File 1-6). The results suggest that these TFs (WRKY, ERF, FAR1 and NAC) are involved in stripe rust resistant of wheat.

Forty-four candidate genes or putative R genes that involve in immune response to *Pst-CYR34* were identified in this study (TableS2). Which mainly include LRR receptor-like serine/threonine protein kinase (Ser/Thr PK), pathogenesis-related protein, disease resistance protein and certain TFs, such as MYB, NAC and WRKY, etc. The relative expression levels of these putative R genes were significant different between L58 and CY12 at both 24hpi and 7dpi. Of those putative R genes, approximately 39% were located on B chromosomes.

Discussion

Plant pathogen is major factors affecting crop yield and quality in world[15]. Plants have evolved pathogen-associated molecular pattern-triggered immunity (PTI) and damage associated molecular patterns that triggered immunity and effector-triggered immunity (ETI), which generate resistance gene products to specifically recognize the effectors releasing from the invader and to confer disease resistance[40]. These two innate immune strategies trigger downstream responses, including the accumulation of reactive oxygen species (ROS) and secondary metabolites to activate the defense systems[41, 42].

Lignin synthesis involved in the stripe rust resistance of wheat

Phenylpropanoid biosynthesis metabolism is the most important secondary metabolic pathway playing a fundamental role in plant defense against biotic (invading pathogens) and abiotic stresses[42]. The main branches of the phenylpropanoid pathway were led to the synthesis of lignin and flavonoid. Although certain researches provided evidence to suggest that lignin, flavonoid and phenolic compounds play important roles during the plant defense response to pathogen, rarely studies on the overall analysis of transcriptome changes of phenylpropanoid biosynthesis genes in wheat. The present results indicated that total gene expression profiles of the phenylpropanoid biosynthesis pathway in response to *Pst-CYR34*. As a result the study focused on the phenylpropanoid biosynthesis pathway with an emphasis on the synthesis and deposition of lignin due to most of enrichment DEGs up-regulated in this pathway (Figure 5A, B). Previous studies have reported that induced lignification is one of several plant defense responses to wounding and to viral or microbial attack[43-46]. In infected plants, lignification and deposition of lignin is a part of the plant cell wall reinforcement that are important processes in the response of plants to restricts pathogen invasion[47-49], and provide a physical barrier to limit pathogen colonization[50].

Induced lignification around the infection centers is generally accompanied by the increased activity of a number of enzymes. Genetic evidence for the role of lignin associated defense is rare, however, either because of the indispensability of lignin for the plant form. In this study, DEGs encoding the enzymes involved in the lignin pathway showed up-regulated expression, which indicated the putative role of lignin in the wheat defense response. More evidence was required to elucidate the definite role of lignin in the wheat defense response to *Pst*. Therefore, the activities of enzymes involved in the phenylpropanoid metabolism pathway and biosynthesis of lignin were measured in this study (Figure 5C, D). POD is involved in the polymerization of monolignols into lignin and reinforcement of the cell wall after pathogen attack and wounding[51]. PAL played an essential role in the phenylpropanoid pathway and has been reported to be responsive to both biotic and abiotic stress, including pathogen attack, wounding, cold and UV stress[52]. Consistent with previous reports, PAL and POD activities were increased as localized lignin deposition[53-55] after *Pst-CYR34* inoculation in both susceptible and resistant wheat seedlings. However, compared with resistant plants, the inoculated susceptible plants showed an obviously slower increase and lower enzyme activities. This result suggests that lignin may be the active form of lignification in HR to protect cells against fungal invasion[44]. Together with the gene expression profiles, we speculated that the most significant difference between susceptible and resistant plants was whether or not the plants could activate the pathway in a timely and efficient manner.

The lignin biosynthetic pathway is initially induced in both resistant and susceptible wheat following rust inoculation[56]. In this study, lignin content was investigated of both resistant and susceptible wheat seedlings after *Pst-CYR34* inoculation. Inoculation of wheat with *Pst-CYR34* increased the total leaves lignin content, which suggested that lignification may be a mechanism through which wheat to restrict the pathogen. An increase in the lignin content was determined in the inoculated resistant wheat (L58) compared with control at both 24h and 7d after *Pst* infection (Figure 5E). Overall, the resistant wheat line displayed increased amounts of lignin concentration was speculated to play a vital role in the wheat

defense response. In accordance with these reports, this result suggested that increased lignification or lignin biosynthesis is critically important for wheat to defense against pathogen invasion.

MAPK signaling pathway and TFs involved in wheat resistance to *Pst-CYR34*

The mitogen-activated protein kinase (MAPK) cascade is a central protein kinase signaling transduction platform, and plays a vital role in connecting receptors/sensors to extracellular and nuclear responses in eukaryotes[57]. MAPKs are typical serine/threonine protein kinases that are also known as extracellular signal regulation kinases[58]. A number of studies have shown that MAPK signal cascades are evolutionary for plant signal transduction which are involved in hormone signaling, plant immunity, regulating growth factors, or damage-associated molecular patterns, and also respond to biotic and abiotic stresses by amplifying the transmitting signal[57, 59]. In this study, the DEGs of RNA-seq results were significantly enrichment in MAPK signal pathway and most of DEGs were up-regulated in this pathway to response *Pst-CYR34* attack at 24h (Figure 7A). Each basic MAPK pathway is minimally composed of three functionally interlinked protein kinases, which are MAPK, MAPK kinase (MAPKK), and MAPK kinase kinase (MAPKKK)[60]. They are linked to upstream receptors and downstream functional targets through a stepwise series of phosphorylation function from MAPKKKs (MEKKs), to MAPKKs (MEKs) to MAPKs (MPKs) that leads to an appropriate output response having high fidelity[61, 62].

MAPK cascade genes have been shown to play vital roles in regulation of plant defense responses. To date, several plant MAPK signaling cascades have been detected in many different species. MAPKKKs are at the beginning of the MAPK cascade and are therefore indispensable. The MAPK cascade was activated after pathogen infection which could further regulate the induction of WRKY33, this result demonstrated the downstream regulation of MAPK cascade could be WRKY transcription factors. Moreover, MAPK (MEKK1-MKK4/5-MPK3/6) cascade signaling networks were induced by FLS2/flg22 perception in plant innate signal transmission immunity to defense pathogens [63, 64]. Firstly, the *Pst* infection could be perceived by FLS2/flg22 like receptor, then with the other signaling transduction, the MAPKKK17 and NDPK1 were induced in different expression pattern between susceptible and resistant wheat cultivars, furthermore the MPK6, MPK3/6 and MPK4/6 were activated by MAPKKK17, NDPK1 or ANP1 which could further activate WRKY33, PR1 and ERF1 (Figure 7B). Then those TFs were regulate gene expression for *Pst* defense response of wheat.

Putative R genes and TFs involved in wheat response to *Pst-CYR34*

Regarding plant defense, MAPK signaling has been shown to function downstream of different types of receptor systems that lead to pathogen associated molecular pattern triggered immunity (PTI) and effector-triggered immunity (ETI)[14, 65]. PTI can be initiated through the toll-interleukin receptor nucleotide binding leucine-rich repeat resistance (TIR) eNB-LRR R protein to driven defense gene expression[66]. ETI can be initiated by the bacterial effector harpin that engages the transcription of the coiled-coil nucleotide binding leucine rich repeat (CC-NB-LRR) [67]. Certain of genes identified as LRR-RLKs and TFs were assayed by RNA-Seq during the wheat defense response to *Pst-CYR34*. Detailed illustration of the response of these EDGs described the interaction effect of signals that allowed the

plant to fine-tune defense responses. Plant RLKs are transmembrane proteins can perceive external signals and initiate signal cascades[68], which control a wide range of bio-processes, including growth, disease resistance, and hormone perception etc. Plant innate immunity depended on the timely perception of the signals, which can be accomplished by pattern recognition receptors (PRRs), including well characterized LRR-RLKs[69]. The identification of groups of LRR-RLKs in the gene expression profiles based on RNA-Seq suggested putative roles for LRR-RLKs in mediating early events in the response of wheat to stripe rust *Pst*. Both up-regulated and down-regulated expression patterns implicated the putative multiple pathways recognized by LRR-RLKs during the wheat immunity.

TFs always play a significant roles by controlling series genes expression to regulate different plant development or response to biotic and abiotic stresses[70]. The majority of TFs, such as WRKY, FAR1, NAC and ER were activated based on the RNA-Seq analysis after pathogen inoculation at 24hpi, which suggested that establishment of the wheat resistance to *Pst-CYR34* require the up-regulation of TFs to modulate the plant immune signaling network.

Conclusions

To better understanding the possibility molecular mechanism of plant-pathogen interaction and to improve plant disease resistant, molecular biology and bioinformatics technology has recent development to made it possible[36]. As a first step in responding to pathogen (*Pst-CYR34*) invasion, wheat plants sense the external signals in a timely fashion, and then signal transduction is conducted by MAPK signaling pathway and other signaling pathways. After signal perception and transduction, subsequent transcriptional activation or inhibition of transcription factors eventually leads to the downstream signal transduction, the plant defense-related genes expression and cell wall reinforcement in wheat to immunity response[19]. In the resistant wheat line, transcripts of all lignin genes were accumulated at 24hpi. A similar expression pattern was reported for methyl unit biosynthetic genes in the same resistant line in a previous study[71]. By combining RNA-seq and biochemical data, it was speculated that DEGs expression levels, enzyme activities, total lignin contents were increased after inoculation. Therefore, a critical role for lignin was deduced to contribute to the wheat disease resistance.

Supplementary Information

Table S1. List of primers used for the relative quantification of gene transcripts (DOCX 17 kb). Table S2. Predicted R genes response associated with *Pst-CYR34* after inoculation (DOCX 17 kb). Figure S1. Weighted gene co-expression network analysis of DEGs in *Pst*-infected wheat young leaves and hub-gene analysis in greenyellow (A) and darkviolet module (B) (DOCX 245 kb). Supplementary File1-1: The data of qRT-PCR (XLSX 52 kb). Supplementary File1-2: The DEGs in KO00940 (XLSX 52 kb). Supplementary File1-3: The DEGs in KO04626 (XLSX 52 kb). Supplementary File1-4: The DEGs in KO04016 (XLSX 52 kb). Supplementary File1-5: KEGG enrichment of greenyellow module (XLSX 52 kb). Supplementary File1-6: The TFs in wheat after *Pst* inoculation (24hpi) (XLSX 52 kb).

Abbreviations

Yr: Stripe rust or yellow rust; Pst: Puccinia striiformis f. sp. Tritici; CY12: Chuanyu12; DEGs: different expression genes; TFs: transcription factors; PTI: pattern-triggered immunity; ETI: effector-triggered immunity; HR: hypersensitivity reaction; WGCNA: Weighted gene correlation network analysis; PAL: ammonia lyase; HCT: hydroxycinnamoyl transferase; CAD: cinnamyl alcohol dehydrogenase; G: guaiacyl; S: syringyl; H: p-hydroxyphenyl.

Declarations

Ethics approval and consent to participate

Not applicable.

Consent for publication

Not applicable.

Availability of data and materials

The dataset and materials presented in the investigation is available by request from the corresponding author.

Competing interests

The authors declare that they have no competing interests. There was no competing Interests in this work.

Funding

This work was supported by the “13th Five-year Plan” for National Key Research and Development (Grant numbers 2017YFD0100902). Innovation Academy for Seed Design, CAS. The “13th Five-year Plan” for Wheat Crops Breeding in Sichuan Province.

Author Contribution statement

LZ and YW provided experimental design and plant material. RL performed experiments and RNA_Seq data analyses. RL and JL were identification phenotype of wheat and data analysis. RL wrote the manuscript. MZ, MD, MXW, JYX, CHZ and YFL were read this article and modified. All authors read and approved the final manuscript.

Acknowledgements

Thanks Cao Shiqin, Jia Qiuzhen and Wang Xiaoming of Gansu Academy of Agricultural Sciences for helping inoculate stripe rust races (*Pst-CYR34*) and identification during seedling stage, and thanks Xia

Xianquan (Sichuan Academy of Agricultural Sciences) for helping to conduct field inoculation.

References

1. Yu M, Mao SL, Hou DB, Chen GY, Pu ZE, Li W, Lan XJ, Jiang QT, Liu YX, Deng M, Wei YM. 2018. Analysis of contributors to grain yield in wheat at the individual quantitative trait locus level. Plant Breeding 137 (1): 35-49. doi:10.1111/pbr.12555
2. Prasad P, Savadi S, Bhardwaj SC, Gangwar OP, Kumar S. 2019. Rust pathogen effectors: perspectives in resistance breeding. Planta 250 (1): 1-22. doi:10.1007/s00425-019-03167-6
3. Zhang H, Yang Y, Wang C, Liu M, Li H, Fu Y, Wang Y, Nie Y, Liu X, Ji W. 2014. Large-scale transcriptome comparison reveals distinct gene activations in wheat responding to stripe rust and powdery mildew. BMC Genomics 15(1). doi:10.1186/1471-2164-15-898.
4. Wellings CR. 2011. Global status of stripe rust: a review of historical and current threats. Euphytica 179 (1):129-141. doi:10.1007/s10681-011-0360-y
5. Wang L, Tang X, Wu J, Shen C, Dai M, Wang Q, Zeng Q, Kang Z, Wu Y, Han D. 2019. Stripe rust resistance to a burgeoning Puccinia striiformis f. sp. tritici race CYR34 in current Chinese wheat cultivars for breeding and research. Euphytica 215 (4). doi:10.1007/s10681-019-2383-8
6. Wan AM, Zhao ZH, Chen XM, He ZH, Jin SL, Jia QZ, Yao G, Yang JX, Wang BT, Li GB, Bi YQ, Yuan ZY. 2004. Wheat stripe rust epidemic and virulence of *Puccinia striiformis* f. sp *tritici* in China in 2002. Plant Disease 88 (8): 896-904. doi:10.1094/pdis.2004.88.8.896
7. Zhou X, Hu T, Li X, Yu M, Li Y, Yang S, Huang K, Han D, Kang Z. 2019. Genome-wide mapping of adult plant stripe rust resistance in wheat cultivar Toni. Theoretical and Applied Genetics 132 (6): 1693-1704. doi:10.1007/s00122-019-03308-1
8. Xu X, Ma L, Hu X. 2019. Overwintering of wheat stripe rust under field conditions in the northwestern regions of China. Plant Disease 103 (4): 638-644. doi:10.1094/pdis-06-18-1053-re
9. Schwessinger B. 2017. Fundamental wheat stripe rust research in the 21st century. New Phytologist 213 (4): 1625-1631. doi:10.1111/nph.14159
10. Wang Y, Xie J, Zhang H, Guo B, Ning S, Chen Y, Lu P, Wu Q, Li M, Zhang D, Guo G, Zhang Y, Liu D, Zou S, Tang J, Zhao H, Wang X, Li J, Yang W, Cao T, Yin G, Liu Z. 2017. Mapping stripe rust resistance gene *YrZH22* in Chinese wheat cultivar Zhoumai 22 by bulked segregant RNA-Seq (BSR-Seq) and comparative genomics analyses. Theoretical and Applied Genetics 130 (10): 2191-2201. doi:10.1007/s00122-017-2950-0
11. Liu TG, Peng YL, Chen WQ, Zhang ZY. 2010. First Detection of virulence in *Puccinia striiformis* f. sp *tritici* in China to resistance genes *Yr24* (=*Yr26*) present in wheat cultivar Chuanmai 42. Plant Disease 94 (9): 1163-1163. doi:10.1094/pdis-94-9-1163c
12. Han DJ, Wang QL, Chen XM, Zeng QD, Wu JH, Xue WB, Zhan GM, Huang LL, Kang ZS. 2015. Emerging *Yr26*-virulent races of *Puccinia striiformis* f. *tritici* are threatening wheat production in the Sichuan basin, China. Plant Disease 99 (6):754-760. doi:10.1094/pdis-08-14-0865-re

13. Bai BB, Liu TG, Liu B, Gao L, Chen WQ. 2018. High relative parasitic fitness of G22 derivatives is associated with the epidemic potential of wheat stripe rust in China. Plant Disease 102 (3): 483-487. doi:10.1094/pdis-04-17-0511-sr
14. Jones JDG, Dangl JL. 2006. The plant immune system. Nature 444 (7117): 323-329. doi:10.1038/nature05286
15. Dodds PN, Rathjen JP. 2010. Plant immunity: towards an integrated view of plant-pathogen interactions. Nature Reviews Genetics 11 (8): 539-548. doi:10.1038/nrg2812
16. Cantu D, Govindarajulu M, Kozik A, Wang M, Chen XM, Kojima KK, Jurka J, Michelmore RW, Dubcovsky J. Next generation sequencing provides rapid access to the genome of *Puccinia striiformis* f. sp *tritici*, the causal agent of wheat stripe rust. Plos One, 2011. 6(8): 1932-6203. doi: 10.1371/journal.pone.0024230
17. Coram TE, Settles ML, Chen XM. Large-scale analysis of antisense transcription in wheat using the Affymetrix GeneChip Wheat Genome Array. BMC Genomics, 2009. 10: 1471-2164. doi: 10.1186/1471-2164-10-253
18. Hulbert SH, Bai J, Fellers JP, Pacheco MG, Bowden RL. 2007. Gene expression patterns in near isogenic lines for wheat rust resistance gene Lr34/Yr18. Phytopathology 97 (9): 1083-1093. doi:10.1094/phyto-97-9-1083
19. Wang X, Liu W, Chen X, Tang C, Dong Y, Ma J, Huang X, Wei G, Han Q, Huang L, Kang Z. 2010. Differential gene expression in incompatible interaction between wheat and stripe rust fungus revealed by cDNA-AFLP and comparison to compatible interaction. BMC Plant Biology 10. doi:10.1186/1471-2229-10-9
20. Zhao J, Zhang H, Yao J, Huang L, Kang ZS. 2011. Confirmation of Berberis spp. as alternate hosts of *Puccinia striiformis* f. sp. *tritic*i on wheat in China. Mygosystema 30 (6):895-900.
21. Yuan FP, Zeng QD, Wu JH, Wang QL, Yang ZJ, Liang BP, Kang ZS, Chen XH, Han DJ. 2018. QTL mapping and validation of adult plant resistance to stripe rust in Chinese wheat landrace Humai 15. Frontiers in Plant Science 9. doi:10.3389/fpls.2018.00968
22. Bai B, Du JY, Lu QL, He CY, Zhang LJ, Zhou G, Xia XC, He ZH, Wang CS. 2014. Effective resistance to wheat stripe rust in a region with high disease pressure. Plant Disease 98 (7):891-897. doi:10.1094/pdis-09-13-0909-re
23. Sharma-Poudyal D, Chen XM, Wan AM, Zhan GM, Kang ZS, Cao SQ, Jin SL, Morgounov A, Akin B, Mert Z, Shah SJA, Bux H, Ashraf M, Sharma RC, Madariaga R, Puri KD, Wellings C, Xi KQ, Wanyera R, Manninger K, Ganzalez MI, Koyda M, Sanin S, Patzek LJ. 2013. Virulence Characterization of international collections of the wheat stripe rust pathogen, Puccinia striiformis f. sp tritici. Plant Disease 97 (3): 379-386. doi:10.1094/pdis-01-12-0078-re
24. Savadi S, Prasad P, Kashyap PL, Bhardwaj SC. 2018. Molecular breeding technologies and strategies for rust resistance in wheat (Triticum aestivum) for sustained food security. Plant Pathology 67 (4):771-791. doi:10.1111/ppa.12802

25. Fuchs M. 2017. Pyramiding resistance-conferring gene sequences in crops. Current Opinion in Virology 26:36-42. doi:10.1016/j.coviro.2017.07.004
26. Zhang S, Wen Z, DiFonzo C, Song Q, Wang D. 2018. Pyramiding different aphid-resistance genes in elite soybean germplasm to combat dynamic aphid populations. Molecular Breeding 38 (3). doi:10.1007/s11032-018-0790-5
27. Bolger AM, Lohse M, Usadel B. 2014. Trimmomatic: a flexible trimmer for Illumina sequence data. Bioinformatics 30 (15):2114-2120. doi:10.1093/bioinformatics/btu170
28. Kim D, Langmead B, Salzberg SL. 2015. HISAT: a fast spliced aligner with low memory requirements. Nature Methods 12 (4):357-U121. doi:10.1038/nmeth.3317
29. Roberts A, Trapnell C, Donaghey J, Rinn JL, Pachter L. 2011. Improving RNA-Seq expression estimates by correcting for fragment bias. Genome Biology 12 (3). doi:10.1186/gb-2011-12-3-r22
30. Trapnell C, Williams BA, Pertea G, Mortazavi A, Kwan G, van Baren MJ, Salzberg SL, Wold BJ, Pachter L. 2010. Transcript assembly and quantification by RNA-Seq reveals unannotated transcripts and isoform switching during cell differentiation. Nature Biotechnology 28 (5):511-U174. doi:10.1038/nbt.1621
31. Anders S, Pyl PT, Huber W. 2015. HTSeq-a Python framework to work with high-throughput sequencing data. Bioinformatics 31 (2): 166-169. doi:10.1093/bioinformatics/btu638
32. Benjamini Y, Hochberg Y. 1995. Controlling the false discovery rate-a practical and powerful approach to multiple testing. Journal of the Royal Statistical Society Series B-Statistical Methodology 57 (1):289-300.
33. Kanehisa M, Araki M, Goto S, Hattori M, Hirakawa M, Itoh M, Katayama T, Kawashima S, Okuda S, Tokimatsu T, Yamanishi Y. 2008. KEGG for linking genomes to life and the environment. Nucleic Acids Research 36: D480-D484. doi:10.1093/nar/gkm882
34. Langfelder P, Horvath S. 2008. WGCNA: an R package for weighted correlation network analysis. BMC Bioinformatics 9. doi:10.1186/1471-2105-9-559
35. dos Santos WD, Ferrarese MDL, Finger A, Teixeira ACN, Ferrarese O. 2004. Lignification and related enzymes in glycine max root growth-inhibition by ferulic acid. Journal of Chemical Ecology 30 (6): 1203-1212. doi:10.1023/B:JOEC.0000030272.83794.f0
36. Xu L, Zhu L, Tu L, Liu L, Yuan D, Jin L, Long L, Zhang X. 2011. Lignin metabolism has a central role in the resistance of cotton to the wilt fungus Verticillium dahliae as revealed by RNA-Seq-dependent transcriptional analysis and histochemistry. Journal of Experimental Botany 62 (15): 5607-5621. doi:10.1093/jxb/err245
37. Kochba J, Lavee S, Spiegelroy P. 1977. Differences in peroxidase-activity and isoenzymes in embryogenic and non-embryogenic shamouti orange ovular callus lines. Plant and Cell Physiology 18 (2): 463-467. doi:10.1093/oxfordjournals.pcp.a075455
38. Schmittgen TD, Livak KJ. 2008. Analyzing real-time PCR data by the comparative C-T method. Nature Protocols 3 (6):1101-1108. doi:10.1038/nprot.2008.73

39. Liu R, Lu J, Zhou M, Zheng SG, Liu ZH, Zhang CH, Du M, Wang MX, Li YF, Wu Y, Zhang L. Developing stripe rust resistant wheat (*Triticum aestivum* L.) lines with gene pyramiding strategy and marker-assisted selection. Genetic Resources and Crop Evolution, 2020. 67: 381–391. doi: 10.1007/s10722-019-00868-5
40. Tang D, Wang G, Zhou JM. 2017. Receptor kinases in plant-pathogen interactions: More than pattern recognition. Plant Cell 29 (4):618-637. doi:10.1105/tpc.16.00891
41. Wu S, Shan L, He P. 2014. Microbial signature-triggered plant defense responses and early signaling mechanisms. Plant Science 228: 118-126. doi:10.1016/j.plantsci.2014.03.001
42. La Camera S, Gouzerh G, Dhondt S, Hoffmann L, Fritig B, Legrand M, Heitz T. 2004. Metabolic reprogramming in plant innate immunity: the contributions of phenylpropanoid and oxylipin pathways. Immunological Reviews 198: 267-284. doi:10.1111/j.0105-2896.2004.0129.x
43. Li C, He Q, Zhang F, Yu J, Li C, Zhao T, Zhang Y, Xie Q, Su B, Mei L, Zhu S, Chen J. 2019. Melatonin enhances cotton immunity to Verticillium wilt via manipulating lignin and gossypol biosynthesis. The Plant journal: for cell and molecular biology. doi:10.1111/tpj.14477
44. Bhuiyan NH, Selvaraj G, Wei Y, King J. 2009. Gene expression profiling and silencing reveal that monolignol biosynthesis plays a critical role in penetration defence in wheat against powdery mildew invasion. Journal of Experimental Botany 60 (2): 509-521. doi:10.1093/jxb/ern290
45. Menden B, Kohlhoff M, Moerschbacher BM. 2007. Wheat cells accumulate a syringyl-rich lignin during the hypersensitive resistance response. Phytochemistry 68 (4): 513-520. doi:10.1016/j.phytochem.2006.11.011
46. Jaeck E, Dumas B, Geoffroy P, Favet N, Inze D, Vanmontagu M, Fritig B, Legrand M. 1992. Regulation of enzymes involved in lignin biosynthesis-induction of O-methyltransferase messenger-RNAs during the hypersensitive reaction of tobacco to tobacco mosaic-virus. Molecular Plant-Microbe Interactions 5 (4): 294-300. doi:10.1094/mpmi-5-294
47. Kauss H, Franke R, Krause K, Conrath U, Jeblick W, Grimmig B, Matern U. 1993. Conditioning of parsley (Petroselinum-crispum L) suspension cells increases elicitor-induced incorporation of cell-wall phenolics. Plant Physiology 102 (2): 459-466. doi:10.1104/pp.102.2.459
48. Uppalapati SR, Marek SM, Lee HK, Nakashima J, Tang Y, Sledge MK, Dixon RA, Mysore KS. 2009. Global gene expression profiling during medicago truncatula-phymatotrichopsis omnivora interaction reveals a role for jasmonic acid, ethylene, and the flavonoid pathway in disease development. Molecular Plant-Microbe Interactions 22 (1): 7-17. doi:10.1094/mpmi-22-1-0007
49. Hu Q, Min L, Yang X, Jin S, Zhang L, Li Y, Ma Y, Qi X, Li D, Liu H, Lindsey K, Zhu L, Zhang X. 2018. Laccase GhLac1 modulates broad-spectrum biotic stress tolerance via manipulating phenylpropanoid pathway and jasmonic acid synthesis. Plant Physiology 176 (2): 1808-1823. doi:10.1104/pp.17.01628
50. Bonello P, Blodgett JT. 2003. Pinus nigra-Sphaeropsis sapinea as a model pathosystem to investigate local and systemic effects of fungal infection of pines. Physiological and Molecular Plant Pathology 63 (5): 249-261. doi:10.1016/j.pmpp.2004.02.002

51. Marjamaa K, Kukkola EM, Fagerstedt KV. 2009. The role of xylem class III peroxidases in lignification. Journal of Experimental Botany 60 (2): 367-376. doi:10.1093/jxb/ern278
52. Huang J, Gu M, Lai Z, Fan B, Shi K, Zhou YH, Yu JQ, Chen Z. 2010. Functional analysis of the Arabidopsis PAL gene family in plant growth, development, and response to environmental Stress. Plant Physiology 153 (4): 1526-1538. doi:10.1104/pp.110.157370
53. Nicholson RL, Hammerschmidt R. 1992. Phenolic-compounds and their role in disease resistance. Annual Review of Phytopathology 30: 369-389. doi:10.1146/annurev.py.30.090192.002101
54. Boyd LA, Smith PH, Foster EM, Brown JKM. 1995. The effects of allelic variation at the Mla resistance locus in barley on the early development of Erysiphe-graminis f. sp. horedi and host responses. Plant Journal 7 (6): 959-968. doi:10.1046/j.1365-313X.1995.07060959.x
55. Caldo RA, Nettleton D, Wise RP. 2004. Interaction-dependent gene expression in Mla-specified response to barley powdery mildew. Plant Cell 16 (9): 2514-2528. doi:10.1105/tpc.104.023382
56. Moerschbacher BM, Noll UM, Flott BE, Reisener HJ. 1988. Lignin biosynthetic-enzymes in stem rust infected, resistant and susceptible near-isogenic wheat lines. Physiological and Molecular Plant Pathology 33 (1): 33-46. doi:10.1016/0885-5765(88)90041-0
57. Xu J, Zhang S. 2015. Mitogen-activated protein kinase cascades in signaling plant growth and development. Trends in Plant Science 20 (1): 56-64. doi:10.1016/j.tplants.2014.10.001
58. Asai T, Tena G, Plotnikova J, Willmann MR, Chiu WL, Gomez-Gomez L, Boller T, Ausubel FM, Sheen J. 2002. MAP kinase signalling cascade in Arabidopsis innate immunity. Nature 415 (6875): 977-983. doi:10.1038/415977a
59. Hoehenwarter W, Thomas M, Nukarinen E, Egelhofer V, Roehrig H, Weckwerth W, Conrath U, Beckers GJM. 2013. Identification of novel in vivo MAP kinase substrates in Arabidopsis thaliana through use of tandem metal oxide affinity chromatography. Molecular & Cellular Proteomics 12 (2): 369-380. doi:10.1074/mcp.M112.020560
60. Zhang T, Liu Y, Yang T, Zhang L, Xu S, Xue L, An L. 2006. Diverse signals converge at MAPK cascades in plant. Plant Physiology and Biochemistry 44 (5-6): 274-283. doi:10.1016/j.plaphy.2006.06.004
61. Mohanta TK, Arora PK, Mohanta N, Parida P, Bae H. 2015. Identification of new members of the MAPK gene family in plants shows diverse conserved domains and novel activation loop variants. BMC Genomics 16. doi:10.1186/s12864-015-1244-7
62. Caunt CJ, Keyse SM. 2013. Dual-specificity MAP kinase phosphatases (MKPs): Shaping the outcome of MAP kinase signalling. Febs Journal 280 (2): 489-504. doi:10.1111/j.1742-4658.2012.08716.x
63. Pitzschke A, Schikora A, Hirt H. 2009. MAPK cascade signalling networks in plant defence. Current Opinion in Plant Biology 12 (4): 421-426. doi:10.1016/j.pbi.2009.06.008
64. Galletti R, Ferrari S, De Lorenzo G. 2011. Arabidopsis MPK3 and MPK6 play different roles in basal and oligogalacturonide- or flagellin-induced resistance against botrytis cinerea. Plant Physiology 157 (2): 804-814. doi:10.1104/pp.111.174003
65. Chang X, Nick P. 2012 Defence Signalling Triggered by Flg22 and harpin is integrated into a different stilbene output in vitis cells. Plos One 7 (7). doi:10.1371/journal.pone.0040446

66. Hilfiker O, Groux R, Bruessow F, Kiefer K, Zeier J, Reymond P. 2014. Insect eggs induce a systemic acquired resistance in *Arabidopsis*. Plant Journal 80 (6): 1085-1094. doi:10.1111/tpj.12707
67. Gopalan S, Wei W, He SY. 1996. Hrp gene-dependent induction of hin1: A plant gene activated rapidly by both harpins and the avrPto gene-mediated signal. Plant Journal 10 (4): 591-600. doi:10.1046/j.1365-313X.1996.10040591.x
68. Gou X, He K, Yang H, Yuan T, Lin H, Clouse SD, Li J. 2010 Genome-wide cloning and sequence analysis of leucine-rich repeat receptor-like protein kinase genes in Arabidopsis thaliana. BMC Genomics 11. doi:10.1186/1471-2164-11-19
69. Panstruga R, Parker JE, Schulze-Lefert P. 2009. SnapShot: Plant immune response pathways. Cell 136 (5): 978-U976. doi:10.1016/j.cell.2009.02.020
70. Singh KB, Foley RC, Onate-Sanchez L. 2002. Transcription factors in plant defense and stress responses. Current Opinion in Plant Biology 5 (5): 430-436. doi:10.1016/s1369-5266(02)00289-3
71. Bhuiyan NH, Liu W, Liu G, Selvaraj G, Wei Y, King J. 2007. Transcriptional regulation of genes involved in the pathways of biosynthesis and supply of methyl units in response to powdery mildew attack and abiotic stresses in wheat. Plant Molecular Biology 64 (3): 305-318. doi:10.1007/s11103-007-9155-x

Table

Table 1 Read statistics in 18 RNA sequencing libraries

Sampe	Raw reads (M)	Clean reads (M)	Q30 (%)	GC (%)	Total mapped (%)	Multiple mapped (%)	Uniquely mapped (%)
CY12_a	49.2±0.03	47.85±0.11	94.8±0.1	54.4±0.6	97.23±0.16	10.3±0.49	86.92±0.35
CY12_b	49.51±0.49	47.97±0.83	94.7±0.4	53.1±0.1	96.61±0.03	8.97±0.23	97.64±0.2
CY12_c	49.56±0.48	48.4±0.41	94.8±0.2	54.1±0.4	97.02±0.17	10.47±0.54	86.55±0.45
L58_a	49.32±0.13	47.76±0.15	94.5±0.3	55.1±0.4	96.95±0.11	10.34±0.06	86.61±0.16
L58_b	49.6±0.3	48.19±0.32	94.4±0.6	53.8±0.4	96.56±0.18	8.63±0.3	87.93±0.12
L58_c	49.61±0.15	47.83±0.54	93.7±0.4	54.5±0.8	96.89±0.18	10.41±1.0	86.48±1.19

a-0hpi, b-24hpi, c-7dpi.

Figures

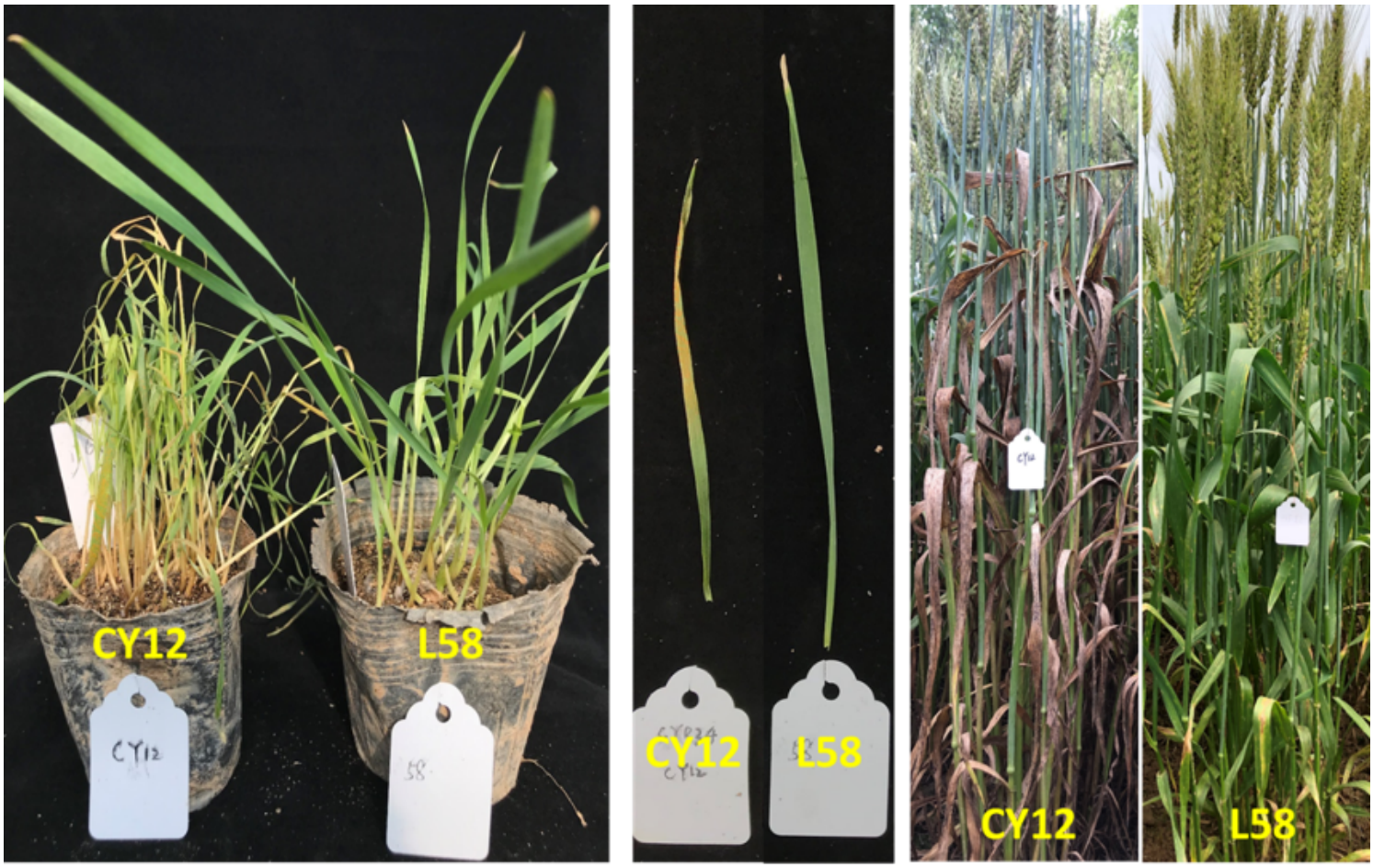

Figure 1

Phenotype identification of two wheat lines with Pst-CYR34 inoculation at 20dpi in greenhouse and adult stage in the field, CY12 is highly susceptible to stripe rust, and L58 is highly resistant to stripe rust pyramiding with Yr10, Yr15, Yr30 and Yr65 on 1B and 3B.

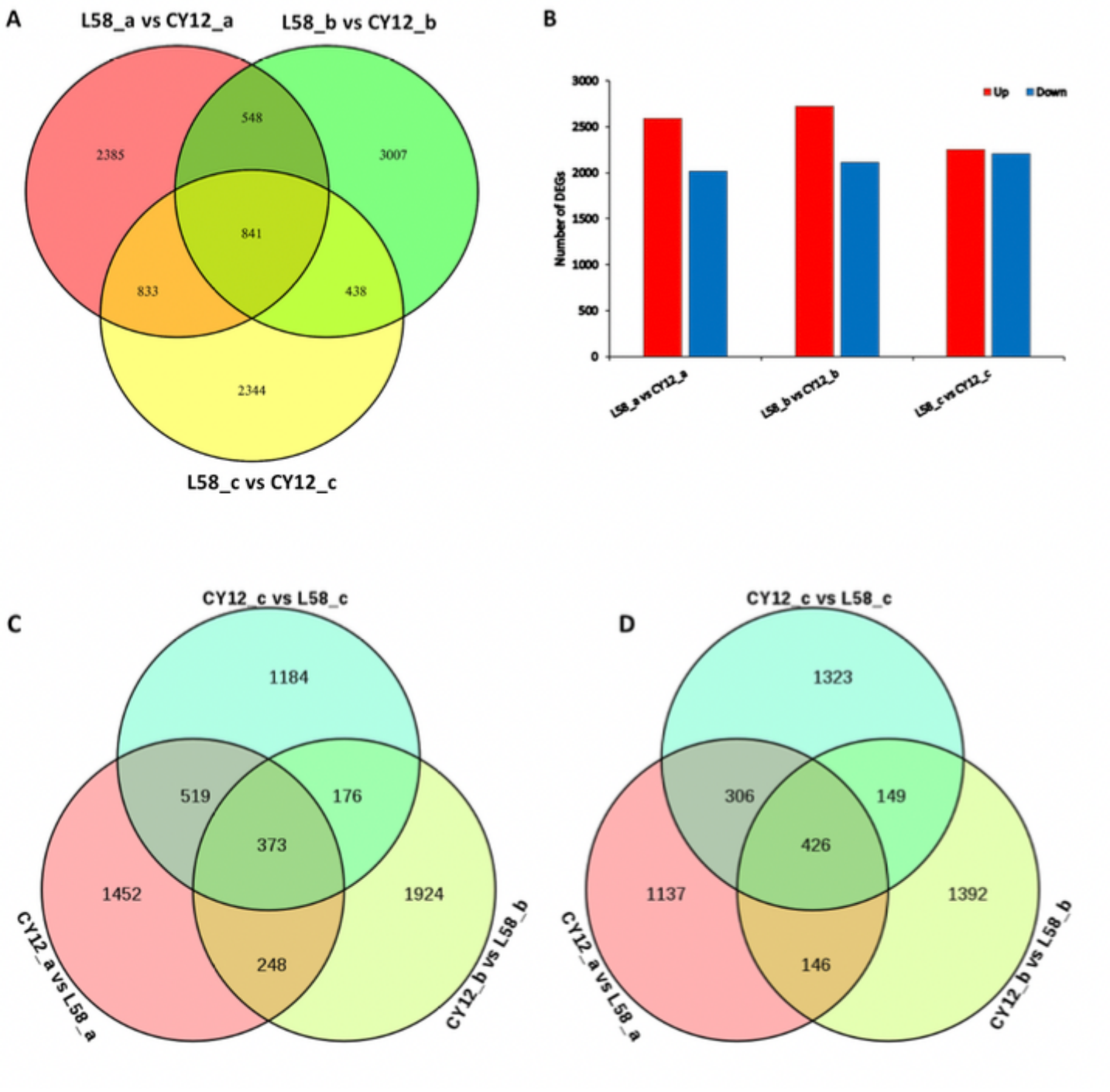

Figure 2

Venn diagrams of differentially expressed genes (DEGs) in CY12 and L58. Venn diagram showing the DEGs between Pst-CYR34 treatment at 0hpi (a), 24hpi (b) and 7dpi (c) time points in CY12 and L58 (A), the number of DEGs up- or down-regulated (B) and the Venn diagrams of up-regulated DEGs (C) and down-regulated DEGs (D) at 0hpi, 24hpi and 7dpi.

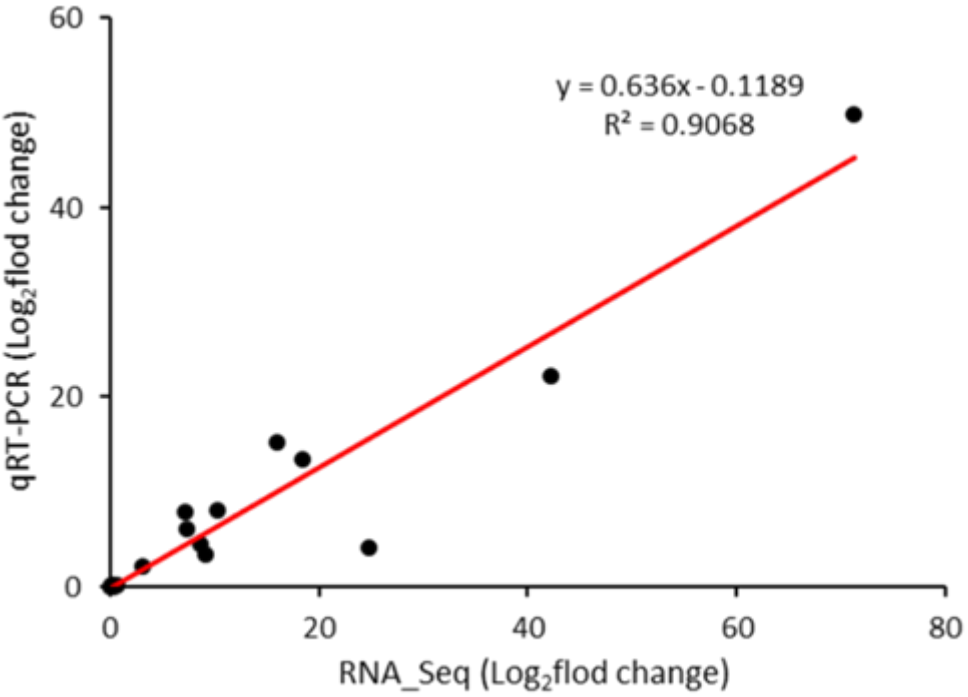

Figure 3

Correlation between qRT-PCR and RNA_seq for the 16 genes. Each point represents a fold change value of expression level between the corresponding Pst-treated at 0hpi (a), 24hpi (b) and 7dpi (c).

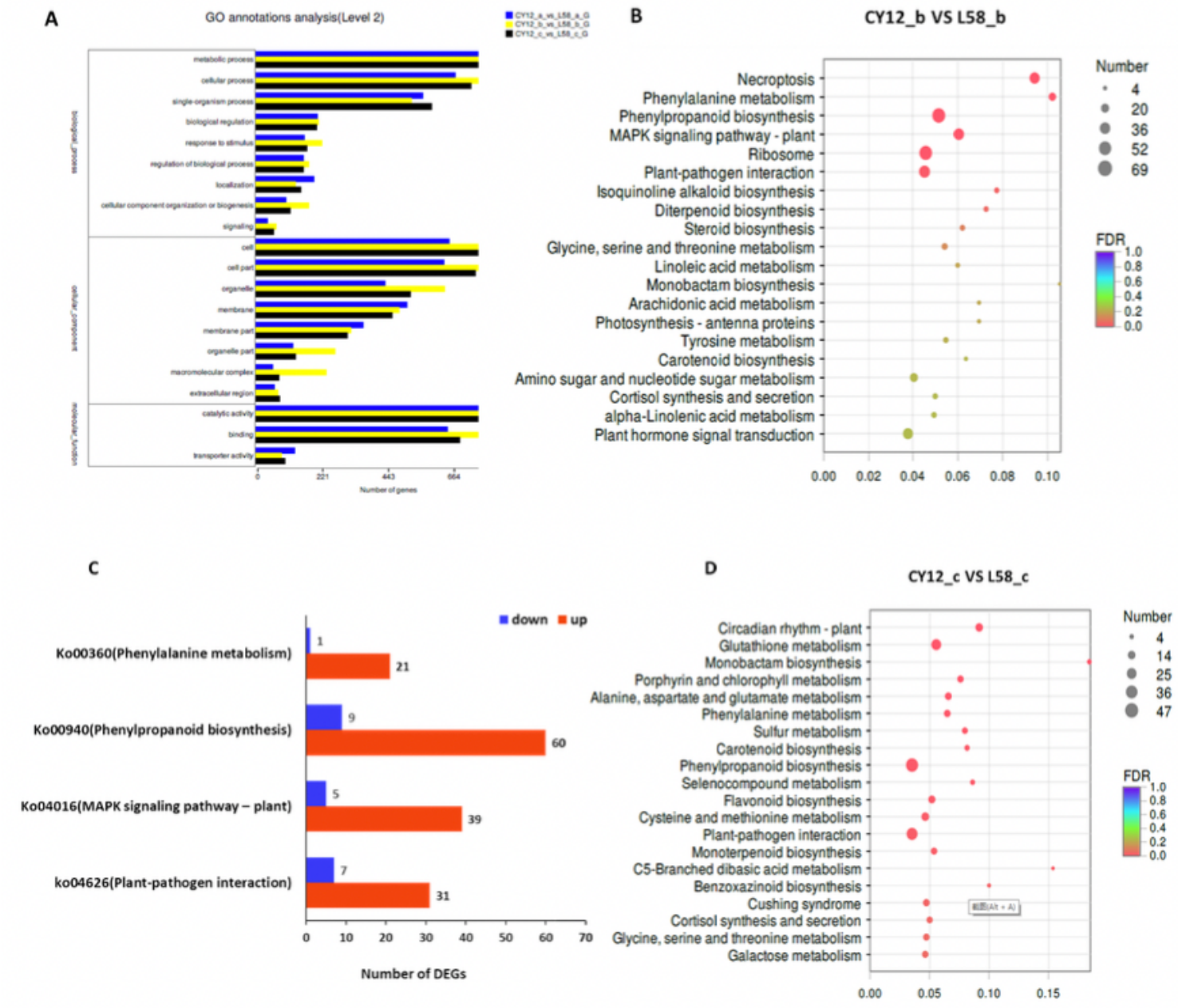

Figure 4

Gene ontology (GO) functional classifications of differentially expressed genes (DEGs) in CY12 and L58 at 0hpi (a), 24hpi (b) and 7dpi (c) time point (A), KEGG analysis of DEGs between CY12 and L58 at 24hpi (B). Number of up- and down-regulated DEGs in phenylanine metabolism, phenylpropanoid biosynthesis, MAPK signaling pathway-plant and plant-pathogen interaction at 24hpi (C), KEGG analysis of DEGs between CY12 and L58 at 7dpi (D).

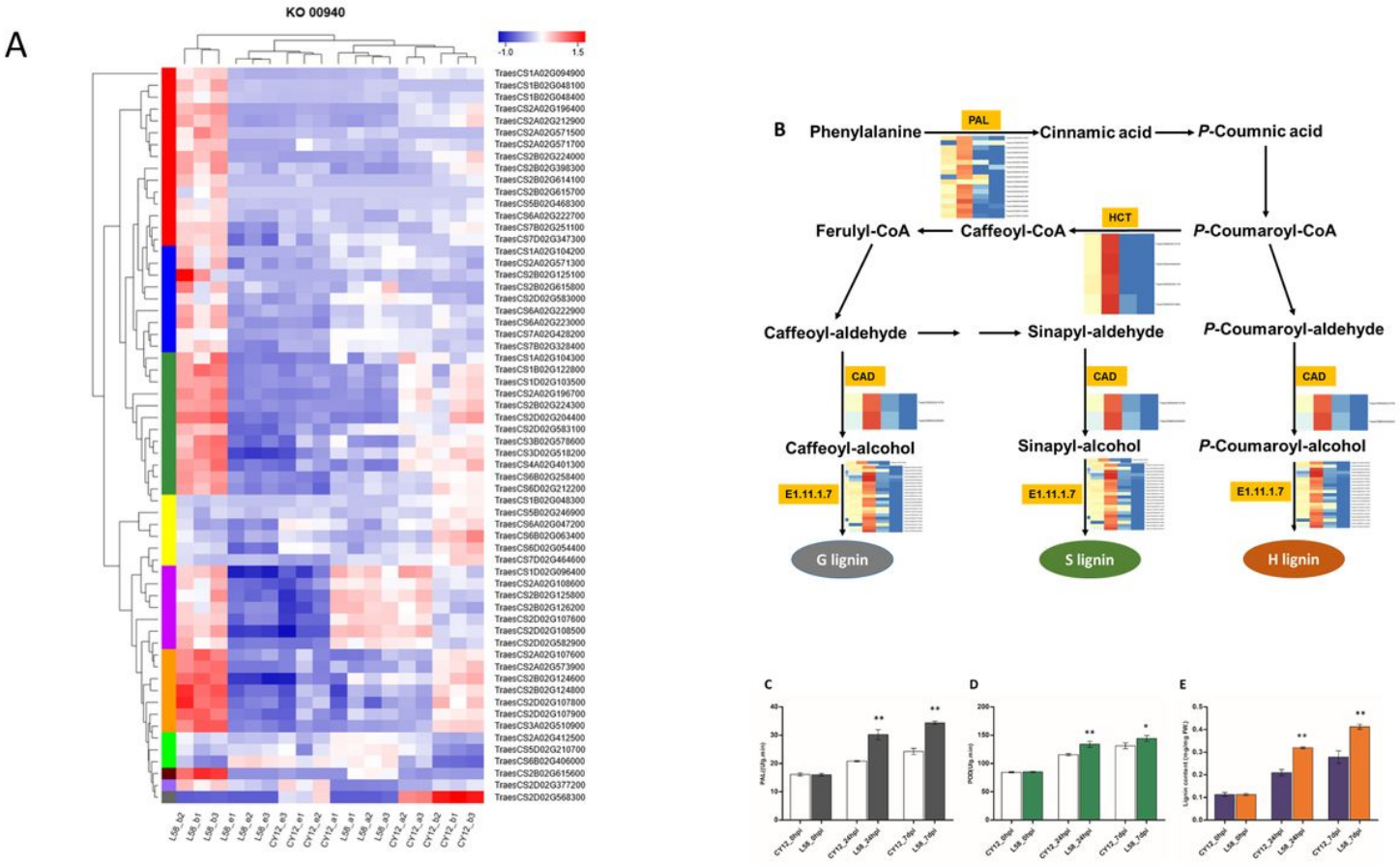

Figure 5

The heat map of expression DEGs enrichment in phenylpropanoid metabolism at 0hpi (a), 24hpi (b) and 7dpi (c) (A) in CY12 and L58 after Pst-CYR34 inoculation, the expression of phenylpropanoid pathway genes after Pst-CYR34 inoculation (B), expression levels are indicated by the heatmap at 0h, 24h and 7d post inoculation, estimated using log2(fold change) for each transcript. PAL, phenylalanine ammonia lyase; HCT, hydroxycinnamoyl transferase; CAD, cinnamyl alcohol dehydrogenase. Enzymes activities of PAL (C) and POD (D) in both two wheat lines at 0hpi, 24hpi and 7dpi; the lignin content in CY12 and L58 after Pst-CYR34 inoculation (E). Each bar are the means ± SD, One-way ANOVA followed by Tukey's significant difference test. *, $P < 0.05$; **, $P < 0.01$.

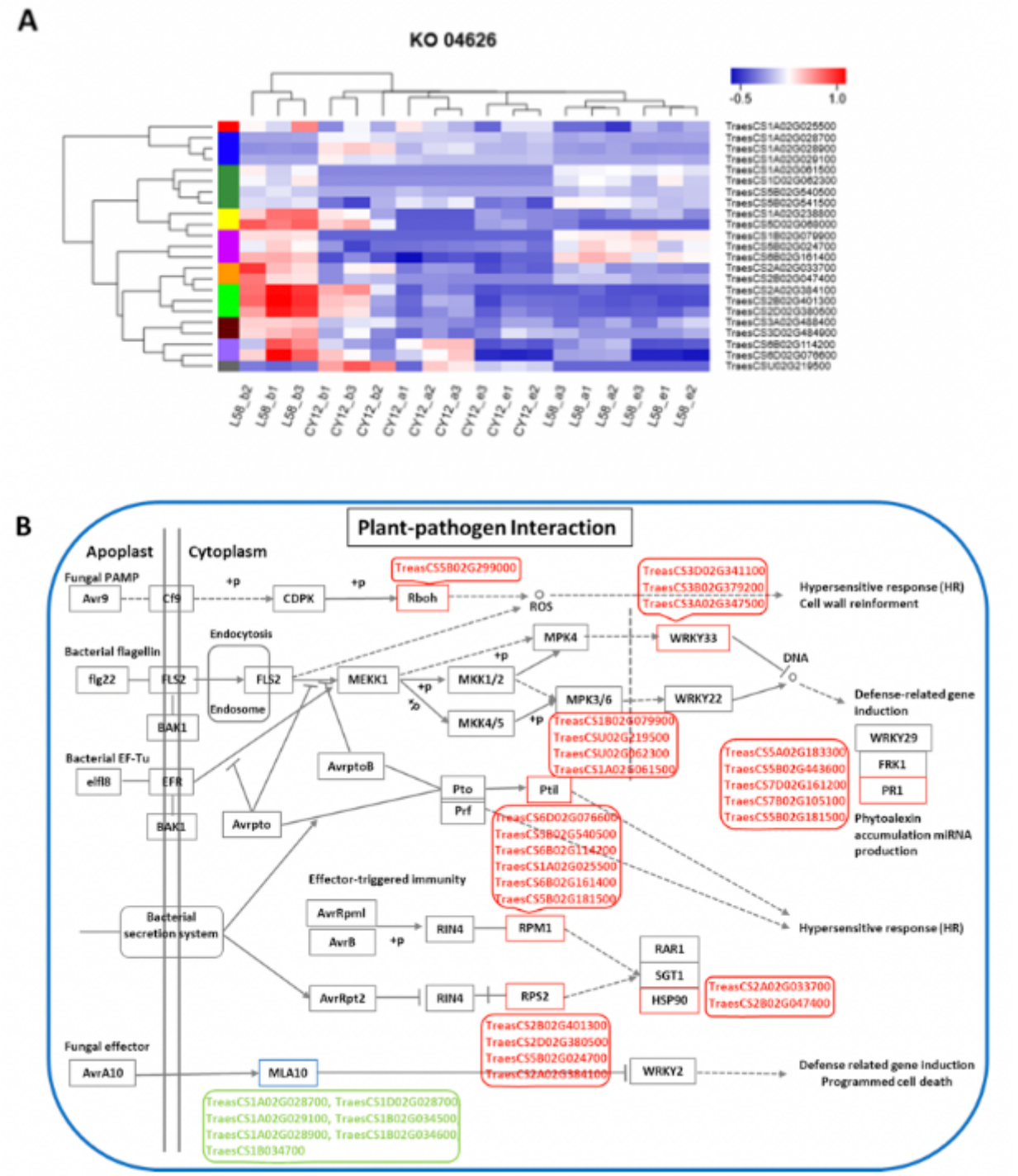

Figure 6

The heat map of expression DEGs enrichment in plant-pathogen interaction at 0hpi (a), 24hpi (b) and 7dpi (c) (A) in CY12 and L58 after Pst-CYR34 inoculation, enriched DEGs expression in plant-pathogen interaction responsible for Pst-CYR34 in CY12 and L58 at 24hpi (B). Genes marked with red indicate up-regulated genes and blue was down-regulated genes in wheat after Pst inoculation at 24hpi.

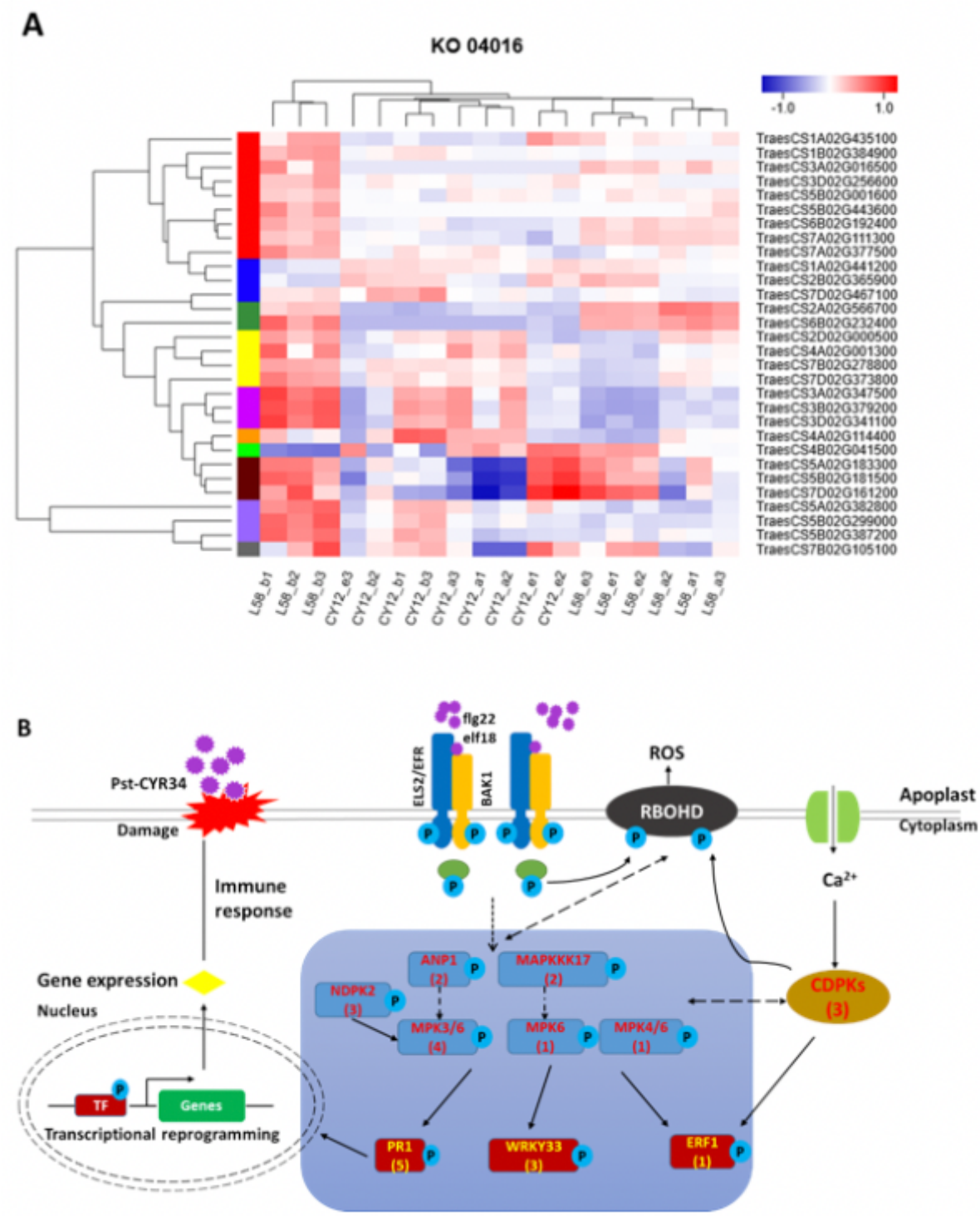

Figure 7

The heat map of expression DEGs enrichment in MAPK signaling pathway at 0hpi (a), 24hpi (b) and 7dpi (c) (A) in CY12 and L58 after Pst-CYR34 inoculation, overview of specially expression DEGs enriched in MAPK signaling pathway triggered by Pst-CYR34 in CY12 and L58 at 24hpi (B). Mitogen-activated protein kinases (MAPKs) and calcium-dependent protein kinases (CDPKs) were triggered by Pst-CYR34 invasion and activated via further phosphorylation cascades target the transcriptional factors (TFs) to regulate resistant gene expression or synthesis of secondary metabolites.

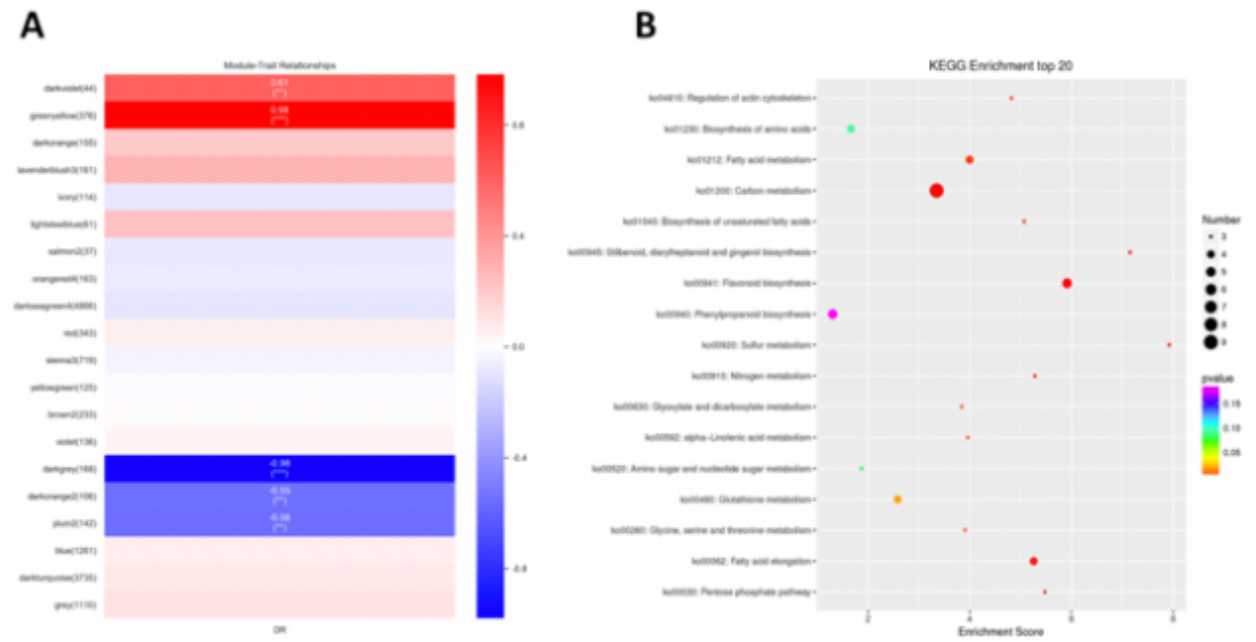

Figure 8

Weighted gene co-expression network analysis of DEGs in Pst-infected wheat young leaves (A). The expressed genes were clustered into 16 modules labeled by different colors (not gray) and the left was number of genes in each module. The value of the correlation between a specific module and sample is indicated by the scale bar on the right. KEGG analysis of module genes in greenyellow (B).

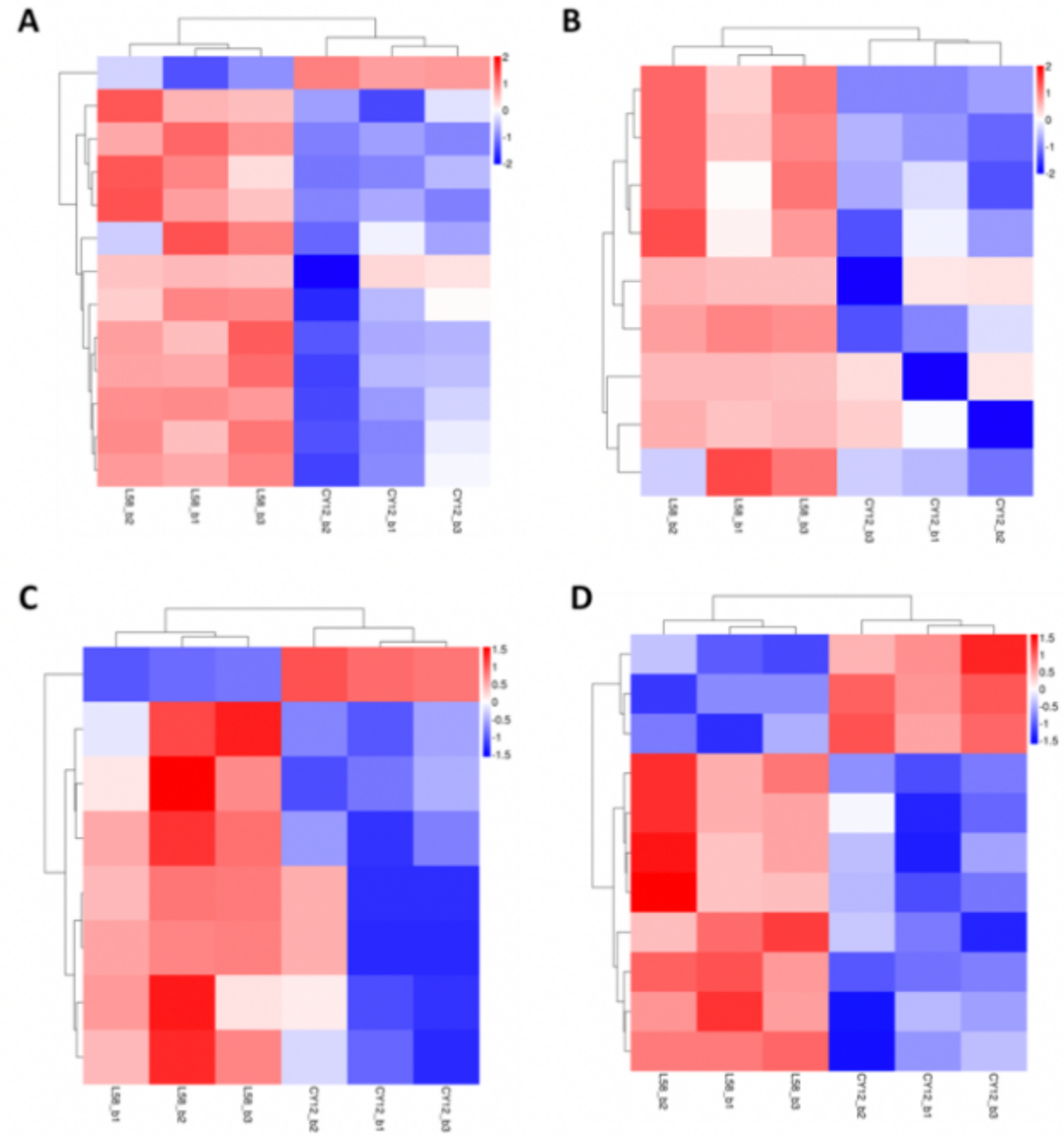

Figure 9

The transcript factors (TFs) in CY12 and L58 after Pst-infection. The TFs including WRKY (A), ERF (B), FAR1 (C) and NAC (D) were triggered by Pst-CYR34 at 24hpi in wheat.

Supplementary Files

This is a list of supplementary files associated with this preprint. Click to download.

- SupplementaryFigures.docx
- SupplementaryTables.docx

- SupplementaryFile1.xlsx